A simple example of a non-Pisot tiling with five-fold symmetry

C. Godrèche, F. Lançon

J. Phys. I France **2** (1992) 207–220 FEBRUARY **1992**, PAGE 207

Classification
Physics Abstracts
61.55 — 61.10D — 02.40

A simple example of a non-Pisot tiling with five-fold symmetry

C. Godrèche([1]) and F. Lançon([2])

([1]) Service de Physique de l'Etat Condensé, Centre d'Etudes de Saclay, 91191 Gif-sur-Yvette Cedex, France
([2]) Département de Recherche Fondamentale sur la Matière Condensée, SP2M/MP, Centre d'Etudes de Grenoble, 38041 Grenoble cedex, France

(Received 31 July 1991, accepted 18 October 1991)

Résumé . — Nous considérons un pavage du plan engendré par une substitution dont la plus grande valeur propre n'est pas un nombre de Pisot. Cette propriété est responsable de l'existence de fluctuations de densité non bornées dans l'espace perpendiculaire, et de l'absence de pics de Bragg dans le spectre de diffraction de la structure. Ce spectre est calculé numériquement à l'aide de relations de récurrence entre amplitudes de Fourier, et comparé à celui du pavage de Penrose.

Abstract . — We consider a tiling of the plane generated by a substitution, the largest eigenvalue of which is not a Pisot number. This property leads to unbounded fluctuations of the density in perpendicular space and to the absence of Bragg peaks in the diffraction spectrum of the structure. This spectrum is computed by means of recursion relations between Fourier amplitudes and compared to that of the Penrose tiling.

1. Introduction.

This paper is the result of two independent lines of research. On one hand, in order to study the stability of quasicrystals, the authors of reference [1, 2] have introduced a two-dimensional model with large and small particles that can be set on the vertices of the Penrose rhombs as shown in figure 1a. In units of $\pi/5$, the Penrose rhombs have corner angles equal to 2 or 3 for the large rhomb and to 1 or 4 for the sharp rhomb. The large particles are set on odd corners and the small particles on even corners. However, it is not possible to decorate the Penrose tiling in such a way because odd and even corners meet at some of its vertices. Therefore other tilings, called binary tilings [3], have been introduced such that at any vertex the corner angles are either all odd or all even. These binary tilings may be crystalline, quasicrystalline or random. With certain pairwise interactions between large and small particles it has been shown that

the binary tiling structures have the lowest potential energy [3]. Firstly, this demonstrates that some quasicrystalline structures can be ground states and not only metastable states. Secondly, and since the binary tilings form a large ensemble, this leads to a model of an entropic quasicrystal [4-6].

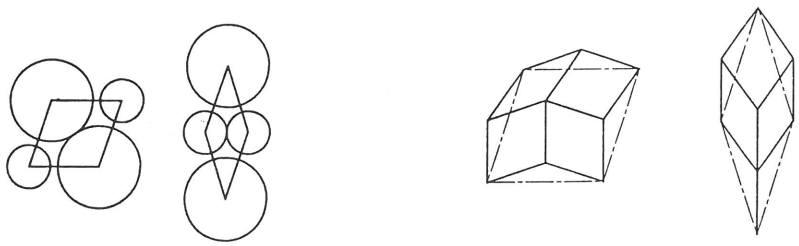

a) b)

Fig. 1. — a) Penrose rhombs decorated with particles of two types. b) Decoration of the Penrose rhombs (dashed lines) with smaller ones (solid lines); this produces binary tilings which can be iterated *ad libitum*.

One possible way to get a binary tiling is to apply the tile decoration shown in figure 1b to any initial tiling built with the two Penrose tiles: Penrose tilings, periodic tilings, random tilings, ..., and also binary tilings [3]. As a consequence, we can iterate this decoration in the same way that Penrose had iterated his inflation rule to get his quasiperiodic tiling [7, 8]. We will show that the tiling we obtain has a different nature [9].

On the other hand, the following line of thought has been pursued. One of the remarkable properties of the Penrose tiling is its diffraction spectrum (or Fourier spectrum) made only of Bragg peaks. In other terms, the tiling is a quasiperiodic structure. It is therefore natural to ask whether there could exist structures, the type of order of which would be intermediate between quasiperiodicity and randomness, with possible more complex Fourier spectra. Reference [10] presents an example of such a structure, in one dimension. This model –named the Circle Structure since it is generated by a circle map–leads to a singular continuous Fourier spectrum. No Bragg peaks exist in the spectrum, nor an absolutely continuous component. This means that its spectral function (or integrated intensity) is a curve analogous to a Devil's staircase, with a zero derivative almost everywhere; hence the spectral density is singular. More generally, structures generated by substitutions (inflation rules) are a good laboratory for the study of these questions. Restricting ourselves, to begin with, to one dimension, it is easy to compute the diffraction spectrum of a structure by writing recursion relations between the Fourier amplitudes. A simple criterion, due to Bombieri and Taylor, gives a necessary and sufficient condition under which the Fourier spectrum of a structure has Bragg peaks [11]. This criterion relies upon the spectral properties of the matrix describing the substitution. If the matrix possesses the Pisot property (stating that apart from the leading eigenvalue, all eigenvalues have moduli less than 1), then the Fourier spectrum contains a discrete component. Conversely, if this not the case, no Bragg peaks appear in the spectrum; therefore, a priori, the spectrum may be a superposition of an absolutely continuous component and a singular continuous one. The case where the substitution matrix does not possess the Pisot property has been called a non-Pisot case and the corresponding structures (tilings) non-Pisot structures (tilings) [12, 13]. The Circle Structure mentioned above is in this respect marginal since it corresponds to the

case where the subleading eigenvalue lies on the unit circle. The generic case where at least two eigenvalues lie outside the unit circle leads to very intricate Fourier spectra [14]. Relying on multifractal analysis of the Fourier spectrum it was claimed in reference [15] that any generic non-Pisot structure (tiling) has a singular continuous Fourier spectrum.

This analysis may be extended to 2D, restricting ourselves to tilings generated by a substitution. In general no section or cut and project method is at our disposal in this case. Nevertheless the spirit of the computation of Fourier amplitudes by recursion relations derived from the substitution is still valid, though in addition geometrical operations on the tiles must be taken into account [16, 17]. As a result the same kind of conclusions on the Fourier spectrum may be derived according to the nature of the substitution, up to additional considerations on the geometry. The first example of a non-Pisot tiling we have been aware of may be found in reference [18]. It is a rather complicated 7-fold symmetric tiling. We then found simple cases of non-Pisot tilings (5-fold or 7-fold symmetric) made of triangles [12].

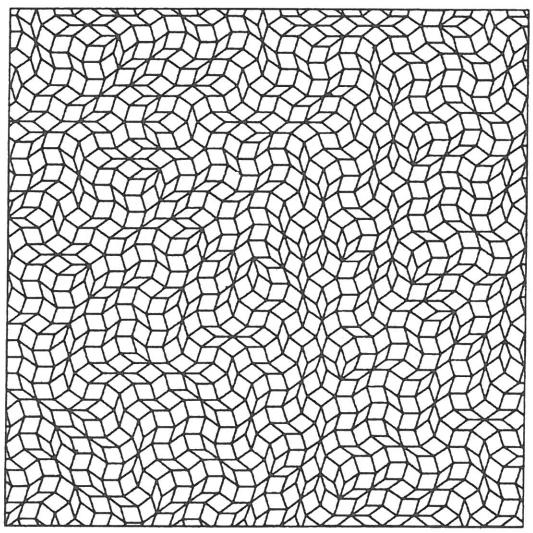

Fig. 2. — The non-Pisot tiling studied in this article.

This paper analyses a very simple non-Pisot 5-fold tiling made of the Penrose rhombs, alluded to in the beginning of this Introduction and shown in figure 2. The convergence of the two independent lines of thought outlined above encouraged us to study such a tiling and to believe in its relevance to physics.

In section 2 we give the definition of the tiling in terms of simple substitution rules. Section 3 is devoted to the study of its main geometrical properties in hyperspace. In section 4, the arguments which show that no Bragg peaks may exist in its diffraction spectrum are exposed; finally a numerical computation of the spectrum is given and compared to that of the Penrose tiling.

2. Substitution rules.

From a decoration to a substitution. In this section we will first emphasize two important properties of the decoration introduced in [3] and shown in figure 1b, namely, that it can be applied to any tiling made of the two Penrose rhombs, and that it produces a new tiling made of the same rhombs at a smaller scale ([1]). Therefore this decoration can be iterated *ad infinitum*. In other words, it leads to a substitution acting on the two Penrose tiles.

Let us consider five unit vectors of the plane in pentagonal directions $\mathbf{e}_k$, $(k = 0, \ldots, 4)$, i.e., the coordinates of $\mathbf{e}_k$ are $(\cos(2\pi k/5), \sin(2\pi k/5))$. The large Penrose rhomb, L, is built on two vectors $\mathbf{e}_0$ and $\mathbf{e}_1$, or those obtained by rotations of angle $2\pi/5$. The sharp rhomb, S, is built on vectors $\mathbf{e}_0$ and $\mathbf{e}_2$, up to the same rotations. The decoration of those two tiles produces new smaller tiles with the same shapes. The five vectors which describe the new tiles are obtained by applying, on the initial unit vectors $\mathbf{e}_k$, a rotation of angle $\pi/10$ and a rescaling by a factor θ^{-1}, where $\theta = 2\sin(2\pi/5) = \sqrt{\tau + 2}$. We denote by $\mathbf{f}_k$, $(k = 0, \ldots, 4)$ these new vectors. They are related to the vectors $\mathbf{e}_k$ by the relations $\mathbf{e}_k = \mathbf{f}_k - \mathbf{f}_{k+2}$.

Let us now show that this decoration may be applied to any tiling made of the two Penrose rhombs, producing a new tiling. Consider the network formed by the tile edges. If the common edge of two adjacent rhombs corresponds to $\mathbf{e}_k$, it transforms into two smaller edges corresponding to $\mathbf{f}_k$ and $\mathbf{f}_{k+2}$ for *both* rhombs. Thus this ensures a perfect match between new rhombs coming from adjacent tiles such that no hole is produced. On the other hand, the two small edges form a boundary line between the new tiles, which are either on one side or the other of the boundary, depending on which of the two initial tiles they come from. Hence there is no overlap between the tiles after a decoration. (This property is not trivial and is no longer true in perpendicular space as will be seen in Fig. 7). Thus starting from any tiling made of Penrose rhombs, a new tiling made of the same tiles at a smaller scale, is produced.

We have therefore proved that this decoration leads to a substitution σ acting on the tiles L and S, which may be summarized (leaving all geometrical considerations aside) as

$$\sigma \left| \begin{array}{l} L \rightarrow LLLS \\ S \rightarrow SSL \end{array} \right. \tag{1}$$

i.e., under one step of substitution a (large) rhomb L gives rise to three L rhombs and one (sharp) rhomb S; an S rhomb gives rise to one L rhomb and two S rhombs. The substitution matrix M relates the numbers of tiles of each type in a tiling before and after one step of substitution:

$$M = \begin{pmatrix} 3 & 1 \\ 1 & 2 \end{pmatrix} \tag{2}$$

The eigenvalues of M are $\lambda_1 = \tau + 2 = \theta^2 \simeq 3.618$ and $\lambda_2 = 3 - \tau = \mu^2 \simeq 1.382$. Note that since λ_1 is not a Pisot number (its conjugate is $\lambda_2 > 1$), θ is not a Pisot number either ([2]). As seen above, under σ, lengths are rescaled by a factor θ^{-1}. We will see in section 3 that μ is also related to a scaling, but in an associated space: the perpendicular space. The frequencies of large and sharp rhombs in the tilings obtained by successive application of the substitution rules on any initial tiling, tend respectively to τ^{-1} and τ^{-2}, which are the components of the

([1]) We will refer to a group of tiles matching perfectly, with no holes and no overlap as a *patch* of tiles or a *finite tiling*. An *infinite tiling* is a patch of tiles which continues to infinity. Depending on the context, a *tiling* will either mean a patch of tiles (finite tiling) or an infinite tiling.

([2]) Let us recall that a Pisot number is an algebraic integer (i.e., a root of an algebraic equation, the coefficient of the term of highest degree of which is equal to 1) whose conjugates have moduli < 1

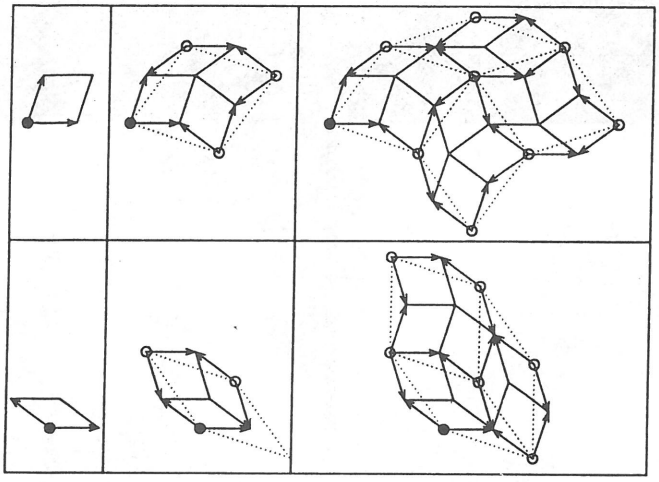

Fig. 3. — Tilings L_n (above) and S_n (below) at iterations $n = 0$, 1 and 2. The inflated tilings $g(L_{n-1})$ and $g(S_{n-1})$ are drawn with dotted lines. Circles and arrows represent the origin and the vectors which characterize each tile. The black disc is set on the plane origin.

right eigenvector associated with the largest eigenvalue λ_1 of M. Note that these frequencies are equal to the frequencies of the L and S tiles in the Penrose tiling.

Geometrical description of the substitution. In the description given above, lengths of the elementary tiles are driven to smaller scales by successive application of the substitution σ on an initial tiling. If one wishes to keep the sizes of the tiles constant one must rescale all lengths by a factor θ, after each substitution. Or one can equivalently introduce another description of the substitution rules where the sizes of the building blocks, namely the two Penrose rhombs, stay constant but where one now sticks those tiles together to form a growing patch of tiles.

Let us give a precise meaning to the geometrical content of this new description of the substitution σ (see [16, 17] for the method used here; [13] contains a preliminary version of the following computation with different geometrical conventions). We consider two sequences of finite tilings (L_n) and (S_n) obtained by iterations of the substitution from the particular initial finite tilings L_0 and S_0 made of one L tile and one S tile respectively. Let us call O the origin in the plane; the vertices of L_0 are located at O, $O + \mathrm{e}_0$, $O + \mathrm{e}_1$ and $O + \mathrm{e}_0 + \mathrm{e}_1$; those of S_0 are located at O, $O + \mathrm{e}_0$, $O + \mathrm{e}_2$ and $O + \mathrm{e}_0 + \mathrm{e}_2$. At step $n + 1$, the finite tilings L_n and S_n are duplicated and joined, with suitable rotations and translations, to create the new tilings L_{n+1} and S_{n+1}:

$$\left| \begin{array}{l} L_{n+1} = L_n + [r, g^{n+1}(\mathrm{e}_0)]L_n + [r^2, g^{n+1}(\mathrm{e}_0 + \mathrm{e}_1)]L_n + [r^3, g^{n+1}(\mathrm{e}_1)]S_n \\ S_{n+1} = S_n + [r^2, g^{n+1}(\mathrm{e}_0 + \mathrm{e}_2)]S_n + [r^4, g^{n+1}(\mathrm{e}_2)]L_n \end{array} \right. \tag{3}$$

where r is a rotation of angle $2\pi/5$ around the origin O; g is a similarity i.e., a rotation of angle $-\pi/10$ around O followed by a dilatation of scaling factor equal to $\theta = \sqrt{\tau + 2}$. The condensed notation [r, t] denotes the product of first the rotation r followed by a translation t applied to a tiling. The symbol + denotes the union operation acting on tilings. When a density of matter is attached to L_0 and S_0 it corresponds to the usual addition of the density functions $L_n(x)$ and $S_n(x)$.

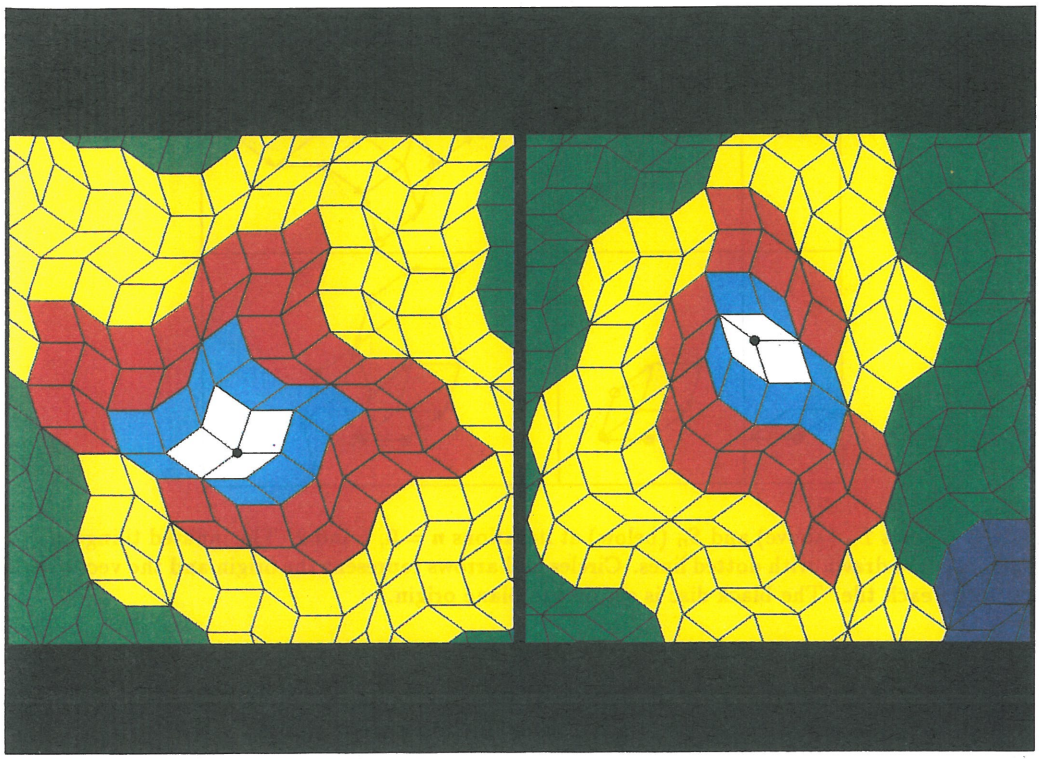

Fig. 4. — Parts of the tilings B_n (left) and D_n (right). The tiles added at each iteration are indicated by a new colour. Tilings at iteration m are invariant parts of tilings at iterations $n \geq m$. The black disc is set on the plane origin.

Since the rotation r and the similarity g commute, relation (3) implies the following recurrence properties: $g(L_n)$ is included in L_{n+1} and $g(S_n)$ in S_{n+1} if $g(L_1)$ is included in L_2 and $g(S_1)$ in S_2. Figure 3 shows that these last conditions are fulfilled (yet they may be not satisfied for decorated tiles, as for instance with atoms at the vertices (Fig. 1a) or with arrows set on the edges). Therefore all the vertices at step n are transformed by g into vertices of the tiling at step $n+1$. This shows that, besides the growth of the tiling, there is an actual inflation property.

Relation (3) also shows that L_n is included in L_{n+1} and S_n is included in S_{n+1}. Therefore, at any step, these tilings contain all their parent tilings at their original positions and with their original orientations. Thus, there is a growing invariant region around the origin O, i.e., a region where the tiles have definitive positions once they have been set. Therefore, if we combine the tilings L_n and S_n around their common origin in such a way that they match perfectly, we also get an invariant tiling centered on O which is no longer at the corner of a finite tiling but now completely surrounded by an invariant region. We consider for instance two new sequences of tilings (B_n) and (D_n) shown in figure 4 and defined by the following equations:

$$\left| \begin{array}{l} B_{n+1} = L_n + [r, \mathrm{O}]L_n + [r^2, \mathrm{O}]L_n + [r^3, \mathrm{O}]S_n \\ D_{n+1} = S_n + [r^2, \mathrm{O}]S_n + [r^4, \mathrm{O}]L_n \end{array} \right. \tag{4}$$

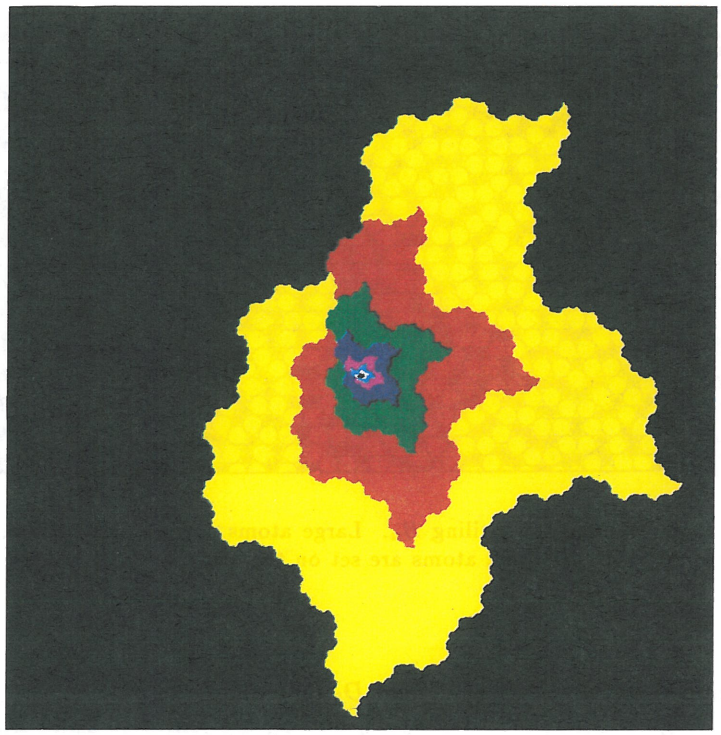

a)

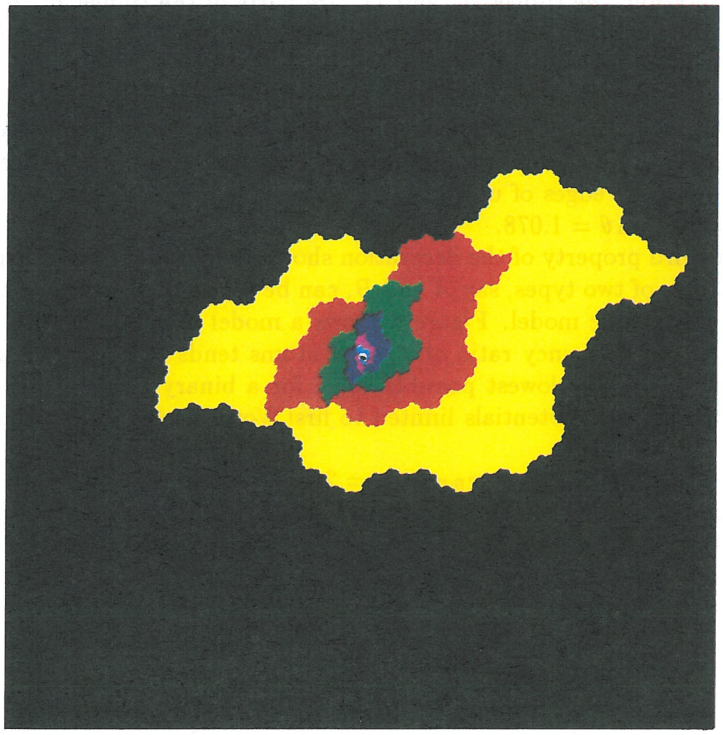

b)

Fig. 5. — Regions covered by B_n (Bear) and D_n (Dog) at iterations n up to 8.

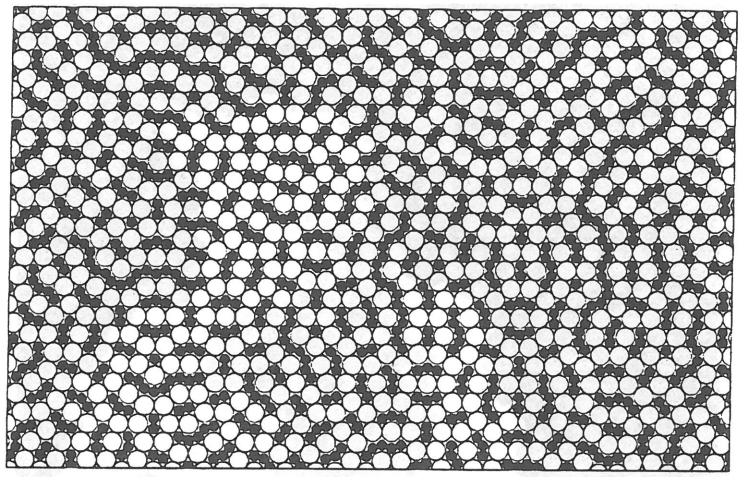

Fig. 6. — Atomic model built with a tiling B_n. Large atoms are set on the vertices where corner angles are equal to $\pi/5$ or $3\pi/5$; small atoms are set on the other vertices (angles equal to $2\pi/5$ or $4\pi/5$).

where O is the null vector. Note that B_1 and D_1 only differ from L_1 and S_1, respectively, by the choice of the origins. Therefore the way L_n and S_n are joined to build B_{n+1} and D_{n+1} is similar to the construction of L_{n+1} and S_{n+1} except for the translations of the origins of the tilings. Up to a rotation, the tilings B_n and D_n are parts of the tilings L_m or S_m for $m > n$

Figure 5 shows the invariant regions, called *B*ear and *D*og, tiled by B_n and D_n respectively, from $n = 1$ to $n = 8$.

As a last remark let us point out that the border of the finite tiling L_n is fractal (the same is true for S_n, B_n, D_n). Consider for example figure 3. At the scale θ^n 4 vertices may be distinguished which form a rhomb 'containing' L_n. 2 consecutive such vertices are separated by a distance θ^n, with 2^n edges of unit length between them. Hence the fractal dimension of the border is $D = \ln 2/\ln\theta = 1.078$.

Binary tilings. A third property of the decoration shown in figure 1a is that it produces binary tilings [3] , i.e., atoms of two types, say A and B, can be set at the vertices of the tilings B_n or D_n to build a dense atomic model. Figure 6 shows a model obtained by this method. When n tends to infinity, the frequency ratio of A to B atoms tends to $\tau/2$. The potential energy of this atomic model has the lowest possible value for a binary two-dimensional alloy if the atomic interactions are pair potentials limited to first Voronoï neighbours and if we have the conditions [3] :

$$r_{AA}/r_{AB} = 2\sin(\pi/5) \;\; ; \;\; r_{BB}/r_{AB} = 2\sin(\pi/10) \;\; ; \;\; \varepsilon_{AB} > \varepsilon_{AA} = \varepsilon_{BB}$$

where $r_{\alpha\beta}$ are the potential minimum positions and $-\varepsilon_{\alpha\beta}$ are the potential minimum values, α and $\beta \in \{A, B\}$. However other structures with the same frequency ratio of A to B atoms have this minimum energy, namely those derived from other binary tilings and for instance quasicrystalline structures.

3. 5D-Hyperspace description.

The tiling under study shares some resemblance with the Penrose tiling. They are both made of the same two rhombs and generated by inflation rules; moreover the infinite tilings have both the same frequencies of tiles. However these two structures appear very different

when described in a five-dimensional space: the vertices of the Penrose tiling are the projections of the vertices of a 5D-cubic lattice contained in a strip of finite width; as shown below this is not true in our case. This implies that the tiling obtained from the substitution rules equation (3) is not quasicrystalline in the usual sense. This assertion will be made more precise below and strengthened in section 4 via consideration of the Fourier spectrum of this tiling.

Each vertex of a tiling made of tiles L and S can be indexed naturally with five integers j_k such that its position in the plane corresponds to $\sum_{k=0}^{4} j_k \mathbf{e}_k$. The integers j_k can be viewed as vertex coordinates of a 5D cubic lattice spanned by the orthogonal vectors $\mathbf{i}_k$ $(k = 0, \ldots, 4)$.

Let R denote the rotation in 5D-space which performs a circular permutation on the vectors $\mathbf{i}_k$. As for the Penrose quasicrystal, we consider the 2D-spaces $E^{\parallel}$ and $E^{\perp}$ and the 1D-space Δ, which are the three sub-spaces globally invariant by the rotation R [19] . Let p be the orthogonal projector onto $E^{\parallel}$ along $E^{\perp} + \Delta$. We identify the 2D physical space with $E^{\parallel}$ so that $p(\mathbf{i}_k) = \mathbf{e}_k$ (since $\|\mathbf{e}_k\| = 1$, $\|\mathbf{i}_k\| = \sqrt{5/2}$).

The large and the sharp rhombs are, respectively, the projection onto $E^{\parallel}$ of 2D-facets defined by $\mathbf{i}_0, \mathbf{i}_1$ and $\mathbf{i}_0, \mathbf{i}_2$ up to circular permutations of the indices. Thus we define, in 5D space, the 2D tiles $\mathcal{L}$ and $\mathcal{S}$ corresponding to the real tiles L and S. Rough 2D surfaces $\mathcal{L}_n$ and $\mathcal{S}_n$ are built in 5D by iteration of a recursion relation similar to (2) and such that $p(\mathcal{L}_n) = L_n$ and $p(\mathcal{S}_n) = S_n$:

$$\left| \begin{array}{l} \mathcal{L}_{n+1} = \mathcal{L}_n + [R, G^{n+1}(\mathbf{i}_0)]\mathcal{L}_n + [R^2, G^{n+1}(\mathbf{i}_0 + \mathbf{i}_1)]\mathcal{L}_n + [R^3, G^{n+1}(\mathbf{i}_1)]\mathcal{S}_n \\ \mathcal{S}_{n+1} = \mathcal{S}_n + [R^2, G^{n+1}(\mathbf{i}_0 + \mathbf{i}_2)]\mathcal{S}_n + [R^4, G^{n+1}(\mathbf{i}_2)]\mathcal{L}_n \end{array} \right. \tag{5}$$

G is equal to $1 - R^2$, where, as mentioned above, R is the circular permutation: $\mathbf{i}_k = R^k(\mathbf{i}_0)$. As for the tilings in the physical plane, all the vertices of $G(\mathcal{L}_n)$ and $G(\mathcal{S}_n)$ are included in $\mathcal{L}_{n+1}$ and $\mathcal{S}_{n+1}$ respectively. The operator G has the same global invariant spaces as R, namely $E^{\parallel}$, $E^{\perp}$ and Δ, and can be represented, in these spaces, by the matrix:

$$M_G = \begin{pmatrix} \theta\cos(-\pi/10) & -\theta\sin(-\pi/10) & 0 & 0 & 0 \\ \theta\sin(-\pi/10) & \theta\cos(-\pi/10) & 0 & 0 & 0 \\ 0 & 0 & \mu\cos(3\pi/10) & -\mu\sin(3\pi/10) & 0 \\ 0 & 0 & \mu\sin(3\pi/10) & \mu\cos(3\pi/10) & 0 \\ 0 & 0 & 0 & 0 & 0 \end{pmatrix} \tag{6}$$

The first block corresponds to $E^{\parallel}$ and represents g, the similarity described in the previous section (a rotation of angle $-\pi/10$ followed by a rescaling by a factor $\theta = \sqrt{\tau + 2}$). The second block corresponds to $E^{\perp}$ and represents a similarity of angle $3\pi/10$ with a scaling factor $\mu = \sqrt{3 - \tau}$. Figure 7 shows the action of the substitution rules in $E^{\perp}$. The last diagonal term is null and corresponds to Δ (the space generated by the vector $\mathbf{i}_0 + \mathbf{i}_1 + \mathbf{i}_2 + \mathbf{i}_3 + \mathbf{i}_4$). Thus all vertices at step n are transformed by G into vertices with a null coordinate along Δ. The other vertices at step $n + 1$ have coordinates equal to $1/\sqrt{2}$ or $2/\sqrt{2}$. Therefore the vertex coordinates along Δ can only have three values, a property satisfied by binary tilings but not by Penrose tilings, where four or five values are possible.

Since the inflation factor in perpendicular space, $\mu \simeq 1.176$, is greater than 1, the vertices are not included in a strip of finite width parallel to a 2D-plane when the number n of substitution steps goes to infinity. Again this property differs from that of Penrose tilings. Figure 8 shows the position density of the vertex projections onto $E^{\perp}$. This curve spreads out more and more on the x axis when n increases, in contradistinction with the usual Penrose case, where it is a fixed window.

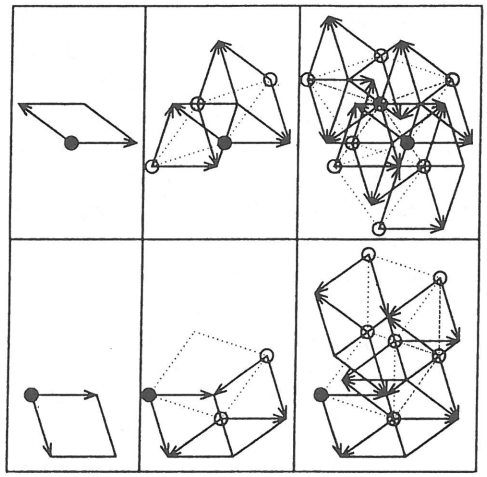

Fig. 7. — Projection onto the perpendicular space $E^{\perp}$ of the surfaces $\mathcal{L}_n$ (above) and $\mathcal{S}_n$ (below) at iterations $n = 0$, 1 and 2. The projection of the inflated surfaces $G(\mathcal{L}_{n-1})$ and $G(\mathcal{S}_{n-1})$ are drawn with dotted lines. Note that the L rhomb corresponds to the S rhomb in perpendicular space $E^{\perp}$ and vice versa. Circles and arrows represent the origin and the vectors which characterize each tile. The black disc is set on the plane origin.

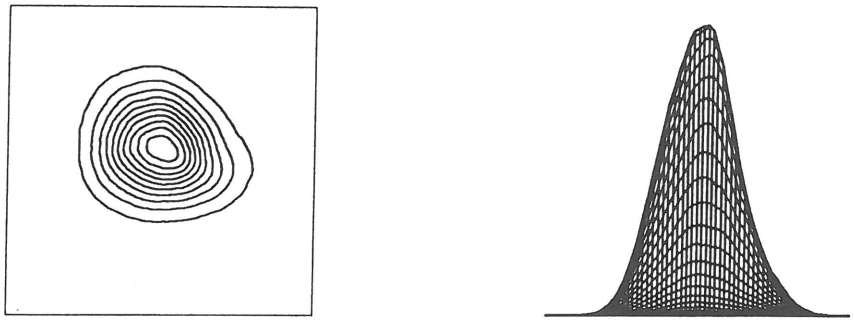

a) b)

Fig. 8. — Contour plot (a) and side view (b) of the density of the perpendicular component of the vertices belonging to $\mathcal{L}_n$ at iteration $n = 11$ (5890625 tiles). The box size in (a) and the abscissa range in (b) are equal to $42.2e$ where e is the length of the tile edges.

4. Fourier spectrum.

One spectacular property of non-Pisot tilings is the absence of Bragg peaks in their diffraction spectra. This may be shown as follows. Let us denote by $\tilde{L}_n(\mathbf{q})$ and $\tilde{S}_n(\mathbf{q})$ the Fourier amplitudes associated to the groups of tiles L_n and S_n, i.e. the Fourier transform of $L_n(\mathbf{x})$ and $S_n(\mathbf{x})$. Since there is no cut-and-project method to generate the tiling under study, the only tool at our disposal to compute its Fourier spectrum relies on recursion relations between

Fourier amplitudes [16, 17], which may be deduced from equations (3). These read

$$\left|\begin{aligned}\tilde{L}_{n+1}(\mathbf{q}) &= \tilde{L}_n(\mathbf{q}) + \exp(-i\mathbf{q}\cdot g^{n+1}(\mathbf{e}_0))\tilde{L}_n(r^{-1}\mathbf{q}) + \\ &\quad \exp(-i\mathbf{q}\cdot g^{n+1}(\mathbf{e}_0+\mathbf{e}_1))\tilde{L}_n(r^{-2}\mathbf{q}) + \exp(-i\mathbf{q}\cdot g^{n+1}(\mathbf{e}_1))\tilde{S}_n(r^{-3}\mathbf{q}) \\ \tilde{S}_{n+1}(\mathbf{q}) &= \tilde{S}_n(\mathbf{q}) + \exp(-i\mathbf{q}\cdot g^{n+1}(\mathbf{e}_0+\mathbf{e}_2))\tilde{S}_n(r^{-2}\mathbf{q}) + \\ &\quad \exp(-i\mathbf{q}\cdot g^{n+1}(\mathbf{e}_2))\tilde{L}_n(r^{-4}\mathbf{q})\end{aligned}\right. \tag{7}$$

These recursion relations should be complemented by initial conditions which depend on the choice of the density of matter on the tiles. We will give an example of particular initial conditions below. Using these recursion relations, it is possible to determine whether there exists a discrete component in the Fourier spectrum, i. e., Bragg peaks. Indeed, in such a case there should exist values of the wavevector $\mathbf{q}$ for which the Fourier amplitudes grow as fast as the size of the system, when the number n of substitution steps increases. In other terms the amplitudes should be proportional to the number of tiles in the sample at generation n. This maximal growth of the amplitudes is achieved generically if and only if all the phases in equations (7) vanish asymptotically mod 2π, for these particular values of $\mathbf{q}$. These conditions yield the following equations on $\mathbf{q}$:

$$\begin{aligned}\mathbf{q}\cdot g^{n+1}(\mathbf{e}_0) &\to 0 \mod 2\pi \\ \mathbf{q}\cdot g^{n+1}(\mathbf{e}_1) &\to 0 \mod 2\pi \\ \mathbf{q}\cdot g^{n+1}(\mathbf{e}_2) &\to 0 \mod 2\pi\end{aligned} \tag{8}$$

These equations may be recast in Cartesian coordinates, writing $\mathbf{q} = q_x\hat{e}_x + q_y\hat{e}_y$. Reminding also that g involves a rescaling by a factor θ, solving equations (8) would mean finding solutions to equations of the type

$$x\,\theta^n \to 0 \mod 1 \quad \text{when} \quad n \to \infty \tag{9}$$

Unfortunately, a theorem due to Pisot [20] asserts that no solution to this equation exists if θ is not a Pisot number. Here $\theta = \sqrt{2+\tau}$, which is not a Pisot number. Hence this proves the absence of Bragg peaks in the Fourier spectrum of the tiling under study [21].

Though the full description of such a spectrum is a difficult open mathematical question, it was conjectured in reference [15] that any non-Pisot structure will have generically a singular continuous spectrum, which, in general, will be rather intricate.

Therefore, we think it illuminating to present the Fourier spectrum of the tiling obtained by iterating numerically the recursion relations (7). We need first to define the initial conditions, or equivalently, the densities of matter on the tiles. We choose to put a delta function on each vertex of a tile, with an amplitude proportional to the angle located at this particular vertex, and such that the total mass on a tile be 1. Hence an atom of unit mass is located at each vertex of the tiling. This choice leads to the following densities

$$\left|\begin{aligned}L_0(\mathbf{x}) &= \frac{2}{10}[\delta(\mathbf{x}) + \delta(\mathbf{x}-(\mathbf{e}_0+\mathbf{e}_1))] + \frac{3}{10}[\delta(\mathbf{x}-\mathbf{e}_0) + \delta(\mathbf{x}-\mathbf{e}_1)] \\ S_0(\mathbf{x}) &= \frac{1}{10}[\delta(\mathbf{x}-\mathbf{e}_0) + \delta(\mathbf{x}-\mathbf{e}_2)] + \frac{4}{10}[\delta(\mathbf{x}) + \delta(\mathbf{x}-\mathbf{e}_0-\mathbf{e}_2)]\end{aligned}\right. \tag{10}$$

In Fourier space this choice yields the following initial conditions on the amplitudes

$$\left|\begin{aligned}\tilde{L}_0(\mathbf{q}) &= \frac{2}{10}[1 + \exp(-i\mathbf{q}\cdot(\mathbf{e}_0+\mathbf{e}_1)] + \frac{3}{10}[\exp(-i\mathbf{q}\cdot\mathbf{e}_0) + \exp(-i\mathbf{q}\cdot\mathbf{e}_1)] \\ \tilde{S}_0(\mathbf{q}) &= \frac{1}{10}[\exp(-i\mathbf{q}\cdot\mathbf{e}_0) + \exp(-i\mathbf{q}\cdot\mathbf{e}_2)] + \frac{4}{10}[1 + \exp(-i\mathbf{q}\cdot(\mathbf{e}_0+\mathbf{e}_2)]\end{aligned}\right. \tag{11}$$

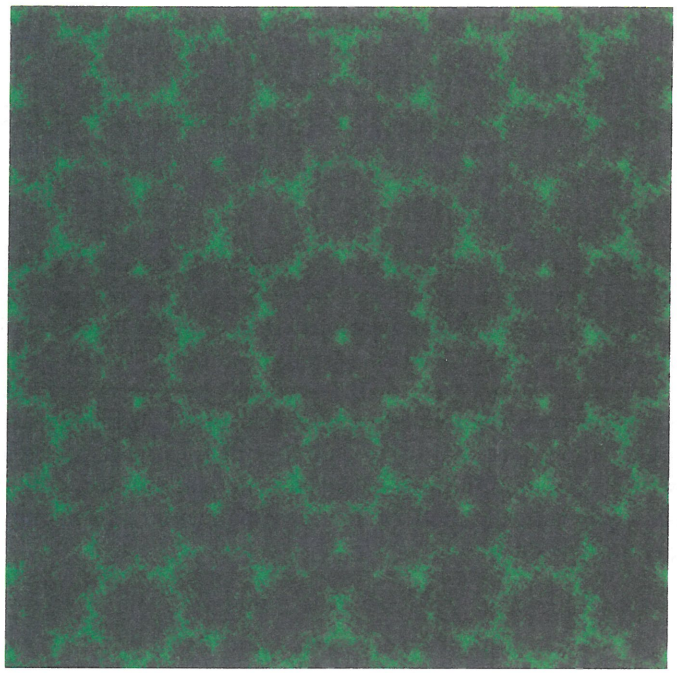

Fig. 9. — Absolute value of the Fourier amplitude $\tilde{L}_6(\mathbf{q})$ computed from equations (7). The plot is done in logarithmic scale. To each pixel is attributed a color going from blue (low amplitude) to green (high amplitude).

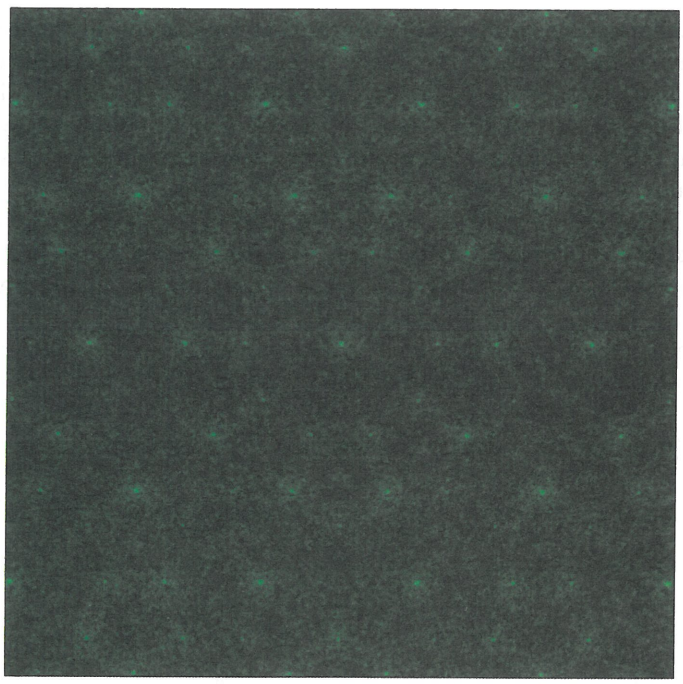

Fig. 10. — Same as figure 9, for the Penrose tiling, at generation $n = 7$.

Figure 9 shows the Fourier spectrum of the tiling, at generation $n = 6$, with $-27 < q_x, q_y < 27$. The picture is made of 512×512 pixels. For comparison, Figure 10 shows the Fourier transform of the Penrose tiling, at generation $n = 7$, using the same method of computation, i.e., using recursion relations between Fourier amplitudes coming from the inflation properties of the tiling [16]. More precisely the tiling used here is made of Robinson triangles, with a unit mass at each vertex; or equivalently of dart and kites with a unit mass at each vertex. As expected, in the case of the non-Pisot tiling under study the intensity is more 'distributed' than in the case of the Penrose tiling.

3. Conclusion.

In this paper we have given the main geometrical properties of a non-Pisot tiling, i.e., a tiling generated by a substitution, the largest eigenvalue of which is not a Pisot number. As seen in the previous sections, this leads to non bounded fluctuations in perpendicular space and to the absence of Bragg peaks in the Fourier spectrum of the structure. Though the rule of construction of this tiling is very simple, its Fourier spectrum is very intricate. More detailed studies of the properties of the spectrum will be the subject of further works. As a final remark let us point out that, in the same way that decagonal phases are related to the Penrose tiling, one may imagine that structures corresponding to the tiling studied in this paper could well be discovered in Nature.

Acknowledgements.

We wish to thank our collaborators L. Billard and J. M. Luck with whom many of the ideas contained in this work have been elaborated.

References

[1] Lançon F., Billard L. and Chaudhari P., *Europhys. Lett.* **2** (1986) 625-629.
[2] Widom M., Stranburg K. J. and Swendsen R. H., *Phys. Rev. Lett.* **58** (1987) 706-709.
[3] Lançon F. and Billard L., *J. Phys. France* **49** (1988) 249-256.
[4] Widom M., Deng D. P. and Henley C. L., *Phys. Rev. Lett.* **63** (1989) 310-313.
[5] Strandburg K. J., Tang L. H. and Jarić M.V., *Phys. Rev. Lett.* **63** (1989) 314-317.
[6] Strandburg K. J., *Phys. Rev. B* **40** (1989) 6071-6084.
[7] Penrose R., *Bull. Inst. Math. Appl.* **10** (1974) 266-271.
[8] Gardner M., *Sci. Am.* **236** (1977) 110-121.
[9] The idea that it could be worth studying the iteration of the decoration described in [3] has been first pointed out to one of us by Michael Widom.
[10] Aubry S., Godrèche C. and Luck J.M., *Europhys. Lett.* **4** (1987) 639; *J. Stat. Phys.* **51** (1988) 1033.
[11] Bombieri E. and Taylor J.E., *J. Phys. France Colloq.* **47** (1986) C3 **19**; *Contemp. Math.* **64** (1987) 241-264.
[12] Godrèche C, and Luck J.M., *Proceedings of the Anniversary Adriatico Conference on Quasicrystals*, Ed. M. V. Jaric and S. Lundqvist, World Scientific (1990).
[13] Godrèche C., *Phase Transitions* **32** (1991) 45.
[14] Godrèche C. and Luck J.M., *Phys. Rev. B* **44** (1991) to be published.

[15] Godrèche C. and Luck J.M., *J. Phys. A* **23** (1990) 3769.
[16] Godrèche C. and Luck J.M., *J. Stat. Phys.* **55** (1989) 1.
[17] Godrèche C., *J. Phys. A* **22** (1989) L1163.
[18] Socolar J., *Quasilattices and Quasicrystals*, PhD thesis, University of Pennsylvania, Philadelphia, (1987).
[19] Duneau M. and Katz A., *Phys. Rev. Lett.* **54** (1985) 2688-2691.
[20] Pisot C., *Ann. Scuola Norm. Sup. Pisa (Italy)* **7** (1938) 205.
[21] New considerations on this topic have recently been developed by Franz Gähler (private communication).